Switching Schemes of the Bidirectional Buck-Boost Converter for Energy Storage System

Ramy Georgious[†] [‡], Sarah Saeed[†], Jorge Garcia[†], Pablo Garcia[†]
[†] Lemur Research Group, Electrical Engineering Dept., University of Oviedo, Gijon, Spain
[‡] Electrical Engineering Dept., University of Port Said, Port Said, Egypt

***Abstract*—This work explores the use of dual-carrier switching modulation schemes for bidirectional buck-boost converters. The buck-boost scheme is utilized as the power converter topology to interface a storage system to a DC-link in electrical vehicles (EVs) and hybrid electric vehicles (HEVs). This topology has the ability to protect the energy storage devices in case of the short-circuit fault at the DC-link. The proposed control strategy decreases the switching losses of the converter under the standard modulation scheme, and also improves the dynamic response of the system by adjusting the static characteristics. The target control is validated through simulations.**

***Index Terms*—bidirectional, buck-boost, energy storage, dual-carrier**

I. Introduction

Energy storage systems (ESSs) have gained a lot of interest in the last few years due to the tendency for enhancing the use of green energy and decreasing emissions. A lot of research has been done in order to integrate the ESSs in electric vehicles (EVs) and hybrid electric vehicles (HEVs). Therefore, several topologies and configurations were introduced in order to utilize these ESSs in EVs and HEVs [1]–[3]. Also, various control schemes were implemented in order to charge and discharge ESSs [4].

One of the basic and common topologies used to connect ESS to a DC-link is the bidirectional boost converter that allows the ESSs to be charged or discharged [5]–[7]. The drawback of this topology is that the ESSs (e.g., battery bank or supercapacitors modules) can suffer from severe damage in the case of a short-circuit fault at the DC-link due to the antiparallel diode of the upper switch [8]. For this reason, a bidirectional buck-boost topology (Fig. 1) is selected in order to protect the ESS and the converter in case of DC-link short-circuit fault [9]. If a short circuit in the DC-link happens, switches will be opened and there is no current can flow from ESS to the DC-link. Another reason for choosing the buck-boost converter is to utilize all the energy of ESSs when their voltages are higher or lower than the DC-link voltage [10]. This gives a degree of freedom when choosing the used ESSs.

In this work, a control scheme that corrects the generation of the duty cycle's values for the boost and buck modes is proposed. The proposed control scheme improves the dynamic response when the converter changes from buck mode to boost mode or vice versa. Also, the proposed control decreases the losses and increases efficiency.

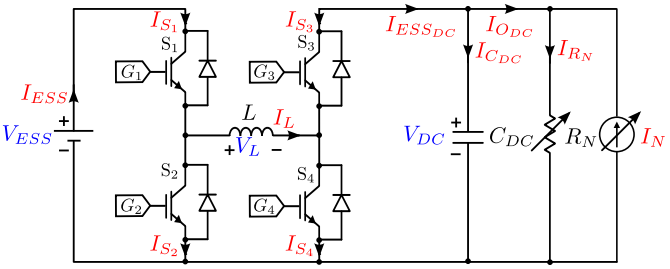

Fig. 1: Bidirectional buck-boost converter attaches the ESS with the DC-link.

This work is organized as follows: Section II studies and analyses the switching schemes in buck and boost modes. After that, Section III proposes the control scheme in order to have a continuous duty cycle and improve the dynamic response of the system. Then, Section IV shows the validation of the proposed control system through simulations. Finally, Section V summarizes the work done and discusses possible future developments.

II. Analysis of the Buck-Boost Switching Scheme

By implementing the buck-boost topology, the switching losses will be doubled, compared to the boost scheme [11]. This is due to the two additional switches in the converter. In order to decrease the switching losses, a dual-carrier modulation is implemented [12]–[17]. One carrier is for the buck mode (varies from 0.0 to 0.5) while the other carrier is for the boost mode (varies from 0.5 to 1.0) [8]. If the converter is operating in a buck mode (Fig. 2), switch S_3 is turned on continuously, and switch S_4 is turned off. Switch S_1 will commutate with the value of the duty cycle while switch S_2 is its compliment. However, in the boost mode (Fig. 3), switch S_4 is switching with the value of duty cycle and switch S_3 is its compliment. In this case, switch S_1 is turned on continuously, and switch S_2 is turned off. So the switching losses cut in half compared to the standard operation of the buck-boost scheme [18]–[20].

Even though theoretically the switching losses of the resulting scheme decrease significantly by using this approach of the dual-carrier modulation; however, it has an important drawback. This disadvantage is derived from the fact that the duty cycle (d) obtained from the control (1), considering the

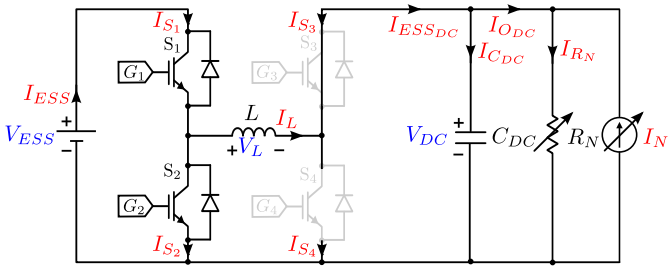

Fig. 2: Bidirectional buck-boost converter operates in buck mode.

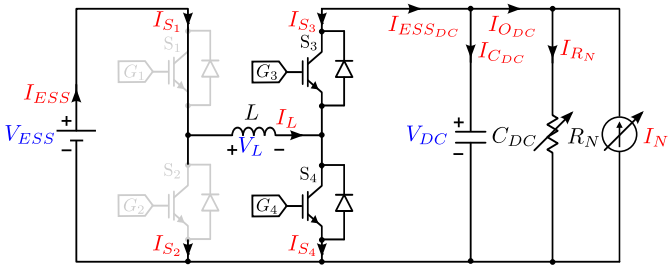

Fig. 3: Bidirectional buck-boost converter operates in boost mode.

buck-boost scheme, does change when applied to the dual-carrier scheme, for both buck and boost operation modes.

$$d = \frac{V_{DC\_meas} + \hat{V}_L}{V_{ESS\_meas} + V_{DC\_meas}} \tag{1}$$

As shown in Fig. 4, if the duty cycle (d) (for S_1 and S_4) derived from the buck-boost, single-carrier scheme is applied directly in the dual-carrier scheme for the buck and boost modes, the switching pattern diverges sensibly. In fact, this target duty cycle (d) should be decreased/increased to achieve the same control action and switching pattern as in the original single-carrier scheme. Therefore, in order to correct this error, an additional adaptation is proposed and implemented. This adaptation modifies the duty cycle to a new value (d_m) before applying to the dual-carrier modulation scheme.

The initial buck-boost scheme presents the original carrier changing from 0.0 to 1.0. Looking at Fig. 4a, the instant at which the control waveform, G, toggles from *turn-on* state to *turn-off* state, t_1, can be calculated as a function of the duty cycle (d) as follows in (2). In the dual-carrier buck mode, a similar calculation would yield to a different instant t_2. In order to maintain t_1 as the instant at which the control waveform, G, toggles from the *turn-on* state to the *turn-off* state, a new value of the duty cycle, d_m, will be established as in (3).

$$t_1 = \frac{d \cdot T_s}{2} \tag{2}$$

$$t_1 = d_m \cdot T_s \tag{3}$$

where d_m is the modified duty cycle for a given switch. From (2) and (3), then the modified duty cycle (d_m) can be

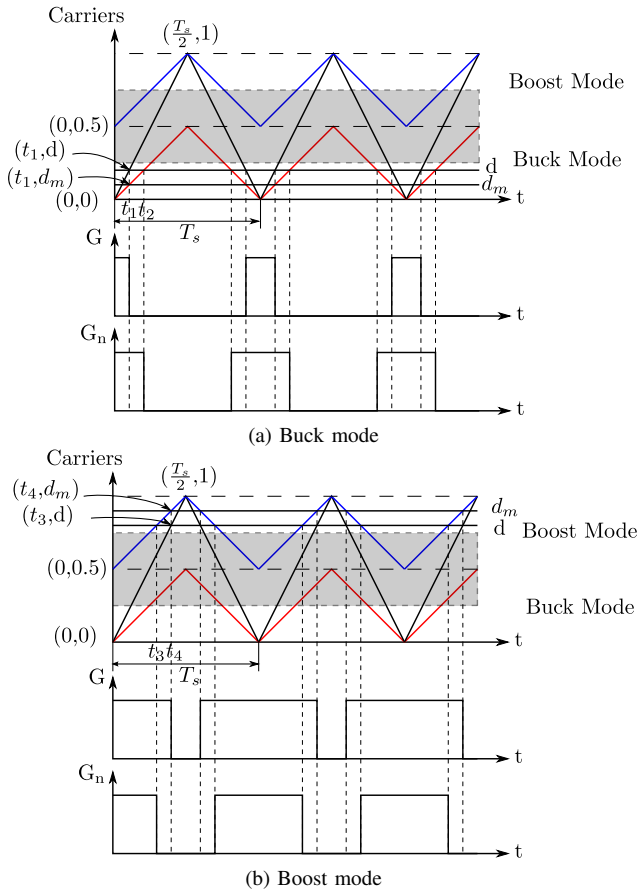

Fig. 4: Switching scheme for the single carrier and the dual-carrier modulations.

obtained as follows in (4).

$$d_m = 0.5d \tag{4}$$

This last equation shows the conversion required to directly apply the buck-boost duty cycle in the dual-carrier scheme, for the buck operation mode. Analogously, Fig. 4b shows a similar error obtained when considering the dual-carrier boost mode. In this case, the duty cycle (d) needs to be increased, in order to provide the same control action applied to the converter.

The new modified duty cycle (d_m) for the boost mode can be calculated by using the same technique as in the previous case. But now, the target instant is t_4 in Fig. 4b as follows in (5). Thus, t_4 can be obtained for this boost mode (6), considering the carrier waveform is taking values from 0.5 to 1.0.

$$t_4 = \frac{dT_s}{2} \tag{5}$$

$$t_4 = (d_m - 0.5)T_s \tag{6}$$

And, from Equations (5) and (6), the following relationship is found in (7).

$$d_m = 0.5 + 0.5d \tag{7}$$

Finally, considering (4) and (7), a final expression for the modified duty cycle can be expressed as in (8). One drawback of this approach is that the operating range of the modified duty is not continuously defined when the converter changes from buck mode to boost mode as can be noticed in (9).

$$d_m = \begin{cases} 0.5d & 0 \leq d \leq 0.5 \quad \text{(buck mode)} \\ 0.5 + 0.5d & 0.5 < d \leq 1 \quad \text{(boost mode)} \end{cases} \tag{8}$$

$$\begin{cases} 0 \leq d_m \leq 0.25 & \text{(buck mode)} \\ 0.75 < d_m \leq 1 & \text{(boost mode)} \end{cases} \tag{9}$$

This means that the range of values from 0.25 to 0.75 is not used. These margins are marked in Figs. 4a and 4b as grey areas. Therefore the resolution of the duty cycle value is smaller than in the previous case as the final available range is half of the original.

Fig. 5 shows the static voltage gain ($\frac{V_{ESS}}{V_{DC}}$) as a function of the duty cycle, in the buck-boost converter, for every operation scheme. It is noticed from Fig. 5 that the gain for the buck operation (magenta line) reaches 1.0 at a duty ratio of 0.25; however, the gain for the boost scheme (green line) reaches 1.0 at a duty ratio of 0.75. This yields to a discontinuity in the duty cycle if using the two-carrier scheme, compared to the original modulation scheme with one carrier only (black line).

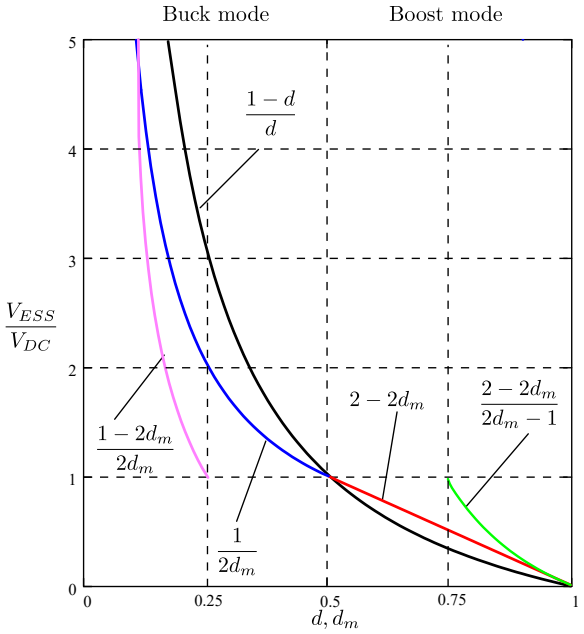

Fig. 5: Static voltage gain of the ESS converter as a function of the duty, for all the control strategies evaluated.

In order to keep the original Pulse Width Modulation (PWM) resolution and increase the resulting operating range (decreasing the grey areas in Fig. 4), and avoid this discontinuity, another approach is followed, that consists of using a different duty cycle calculation for either the buck or the boost modes.

III. Proposed Control by Changing Duty Cycle Calculation

In this strategy, the control action is going to be tailored for the operation case, and therefore no additional adjustment on the duty cycle needs to be undertaken. The duty cycle, d, is going to be applied for the buck mode and the boost mode, the following relationships can be found in (10) and (11).

$$d_1 = \frac{V_{DC\_meas} + \hat{V}_L}{V_{ESS\_meas}} \tag{10}$$

$$d_2 = \frac{V_{DC\_meas} - V_{ESS\_meas} + \hat{V}_{L_1}}{V_{DC\_meas}} \tag{11}$$

And from these expressions, the value that is actually going to be compared to the dual-carrier scheme, defined in (8), needs to be calculated as in (12). It is worthy to notice that in this case, the transformation does not imply a loss in the resolution as the available duty ratio margin is again the full region (from 0.0 to 1.0).

$$d_m = \begin{cases} d_1 & 0 \leq \dfrac{V_{DC\_meas}}{V_{ESS\_meas} + V_{DC\_meas}} \leq 0.5 \\ d_2 & 0.5 < \dfrac{V_{DC\_meas}}{V_{ESS\_meas} + V_{DC\_meas}} \leq 1 \end{cases} \tag{12}$$

Figure 5 shows the continuity of the duty cycle by using this proposed approach. The gain in buck mode (blue line) reaches unity at 0.5, and the gain in boost mode (red line) reaches unity exactly at 0.5. This yields a final modification in the *Duty Cycle Calculation Block*, as it is depicted in Fig. 6. As it can be noticed from Fig. 6, the duty cycle modification depends on the buck-boost duty cycle in steady-state (13).

$$d_{ESS\_ss} = \frac{V_{DC\_meas}}{V_{ESS\_meas} + V_{DC\_meas}} \tag{13}$$

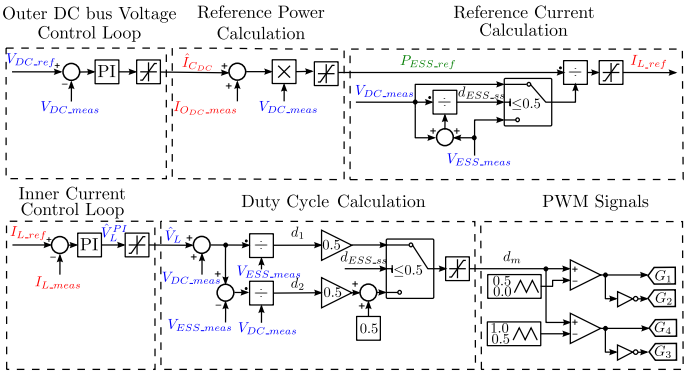

Fig. 6: Proposed control scheme for the bidirectional buck-boost converter in order to maintain the DC-link voltage constant.

As can be seen, the inductor current reference of the converter ($I_{L_{ref}}$) changes depending on the mode of operation (buck or boost). In buck mode, the inductor current reference is equal to the output current of the converter at the DC

side. However, for boost operation mode, this inductor current reference equals the ESS device's current reference. This can be summarized as in (14).

$$I_{L\_ref} = \begin{cases} \dfrac{P_{ESS\_ref}}{V_{DC\_meas}} & d_{ESS\_ss} \leq 0.5 \text{(Buck mode)} \\ \dfrac{P_{ESS\_ref}}{V_{ESS\_meas}} & d_{ESS\_ss} > 0.5 \text{(Boost mode)} \end{cases} \quad (14)$$

IV. Simulation Results

The aim of the control scheme in Fig. 6 is to regulate the DC bus voltage to a constant value. In order to demonstrate the transition from buck mode to boost mode, the DC bus voltage reference (V_{DC_ref}) will change from buck mode (50V) to boost mode (200V) at 0.5s and then back to buck mode (50V) at 0.7s, considering ESS (i.e. supercapacitor) which has 96V nominal voltage. Table I shows the parameters of the bidirectional buck-boost converter used in the simulations. The control parameters are presented in Table II. The PI controller of the voltage and current control loops is in the ideal form.

TABLE I: Parameters of the bidirectional buck-boost converter.

Parameter	Symbol	Value
Nominal ESS voltage	V_{ESS}	96 V
ESS energy	E_{ESS}	106 Wh
ESS rated capacitance	C_{ESS}	82.5 F
Capacitance of the DC bus	C_{DC}	470 μF
Inductance of the inductor	L	3.6 mH
Series Resistance of the inductor	R_L	0.08 Ω

TABLE II: Parameters of the proposed control scheme.

Parameter	Symbol	Value
DC Bus Voltage Control Loop		
Bandwidth	Bw_v	30 Hz
Proportional gain	K_{p_v}	0.0886
Integral time	T_{i_v}	0.0188 s
Current Control Loop		
Bandwidth	Bw_i	300 Hz
Proportional gain	K_{p_i}	6.7670
Integral time	T_{i_i}	0.0422 s
PWM Signals		
Switching frequency	f_s	20 kHz
Dead time	t_d	1 μs

The simulation results are obtained from three different control schemes: 1) Original control with a single carrier, 2) Modified control with dual-carrier, 3) Proposed control with dual-carrier, in order to compare between them. The proposed control provides a faster response of the DC bus voltage (green line) compared to the other two controls as depicted in Fig. 7. This is due to the continuity of the duty cycle during the transition from the buck mode to the boost mode and vice versa as can be noticed in the zoom of the duty cycle.

Figure 8 shows the switching schemes of the dual-carrier modulation of the proposed control during both buck and boost modes. As can be seen from Fig. 8 that switch S_3 is turned on continuously and switch S_4 is turned off in the Buck mode; however, in the boost mode switch S_1 is turned on continuously and switch S_2 is turned off. This results in a decrease in the switching losses and an increase in converter efficiency.

The calculation of the losses is done for a given set of operating conditions. The converter is working in the steady-state case and the DC is controlled to a reference voltage of 200 V and the load power is 1 kW. The total switching and conduction losses using the original method were computed to be 21.44W, which is higher compared to the proposed control scheme with dual-carrier which resulted in 9.75W losses.

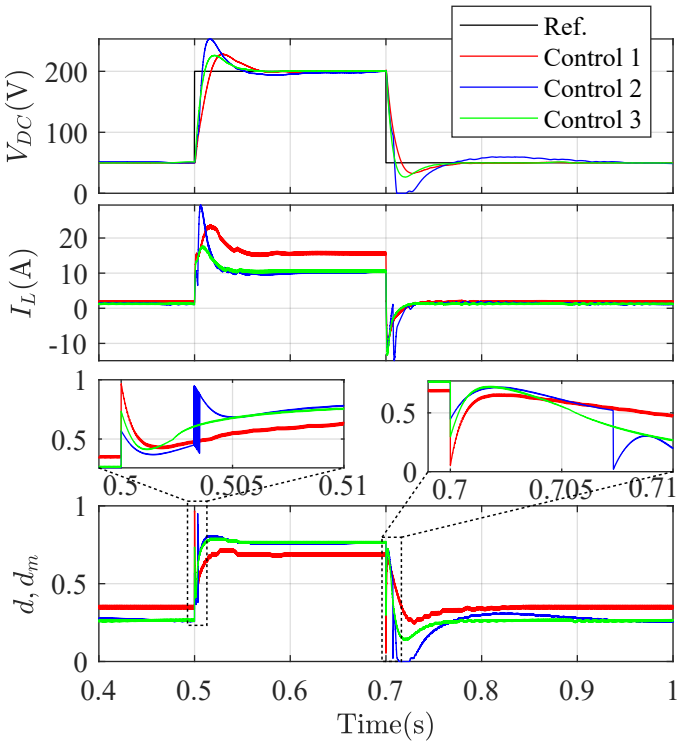

Fig. 7: DC bus voltage reference is changed at 0.5s from 50V (buck mode) to 200V (boost mode) and then back to 50V (buck mode) at 0.7s.

V. Conclusions

An analysis of a dual-carrier switching pattern control scheme for a bidirectional buck-boost converter has been carried out, showing that the proposed control has better dynamics and a faster response solving the problem of discontinuity of the duty cycle in dual-carrier modulation. In addition to that, the proposed control has fewer losses compared to the original control with a single carrier. Simulation demonstrations, in MATLAB/Simulink, of the control schemes are presented to validate the behavior of the control.

Future developments include the implementation of the proposed control scheme with different ESSs. Also, different

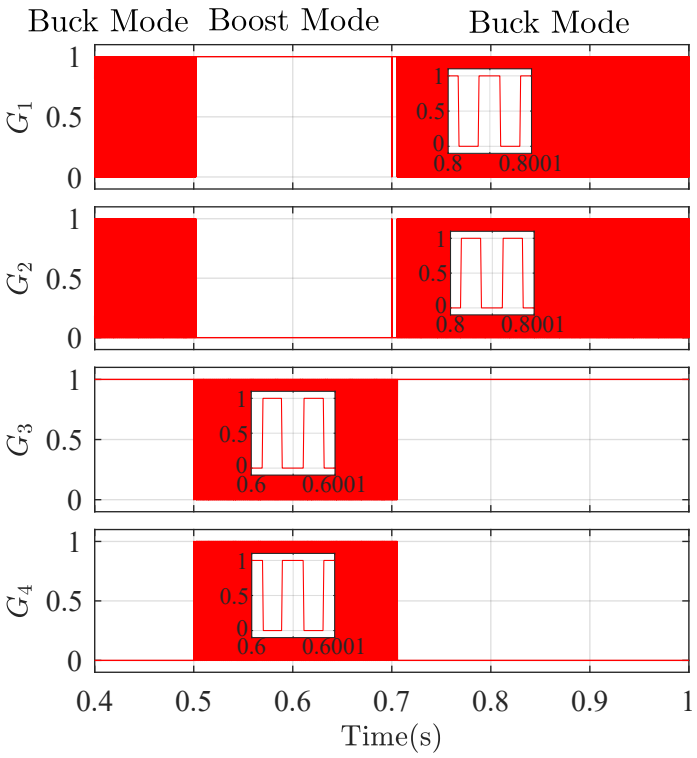

Fig. 8: Switching schemes of the proposed control during the transition from buck mode to boost mode and back to buck mode again.

switches (e.g. wide band-gap devices) will be taken into account in the bidirectional buck-boost converter.

Acknowledgments

This work has been partially funded from the European Union's H2020 Research and Innovation program under grant agreement 864459 , Project "Cost Effective Technological Developments For Accelerating Energy Transition (TALENT)". This wok has been partially supported by the Spanish Government, Innovation Development and Research Office (MEC), under research grant ENE2016-77919, Project "Conciliator", and research grant PID2019-111051RB-100 Project "B2B-Energy", and by the European Union through ERFD Structural Funds (FEDER). This work has been partially supported by the government of Principality of Asturias, Foundation for the Promotion in Asturias of Applied Scientific Research and Technology (FICYT), under Grant FC-GRUPIN-IDI/2018/000241 and Severo Ochoa research grants, PA-13-PF-BP13-138 and PF-BP16-133.

References

[1] Z. Amjadi and S. S. Williamson, "Power-electronics-based solutions for plug-in hybrid electric vehicle energy storage and management systems," *IEEE Transactions on Industrial Electronics*, vol. 57, no. 2, pp. 608–616, Feb 2010.

[2] T. P. Kohler, D. Buecherl, and H. Herzog, "Investigation of control strategies for hybrid energy storage systems in hybrid electric vehicles," in *2009 IEEE Vehicle Power and Propulsion Conference*. IEEE, sep 2009, pp. 1687–1693.

[3] C. Pinto, R. de Castro, J. V. Barreras, R. Esteves Araujo, and D. A. Howey, "Smart balancing control of a hybrid energy storage system based on a cell-to-cell shared energy transfer configuration," in *2018 IEEE Vehicle Power and Propulsion Conference (VPPC)*. IEEE, aug 2018, pp. 1–6.

[4] R. Mishra and R. Saxena, "Comprehensive review of control schemes for battery and super-capacitor energy storage system," in *2017 7th International Conference on Power Systems (ICPS)*. IEEE, dec 2017, pp. 702–707.

[5] Z. Amjadi and S. S. Williamson, "Novel control strategy design for multiple hybrid electric vehicle energy storage systems," in *2009 Twenty-Fourth Annual IEEE Applied Power Electronics Conference and Exposition*, 2009, pp. 597–602.

[6] Rae-Young Kim, Chang-Soon Lim, Hong-Joo Jung, and Soon-Bong Cho, "A general-purpose integrated battery energy module for non-isolated energy storage system applications," in *2012 IEEE Vehicle Power and Propulsion Conference*. IEEE, oct 2012, pp. 1503–1507.

[7] A. L. Allègre, R. Trigui, and A. Bouscayrol, "Different energy management strategies of hybrid energy storage system (hess) using batteries and supercapacitors for vehicular applications," in *2010 IEEE Vehicle Power and Propulsion Conference*. IEEE, sep 2010, pp. 1–6.

[8] R. Georgious, J. Garcia, P. Garcia, and M. Sumner, "Analysis of hybrid energy storage systems with DC link fault ride-through capability," in *2016 IEEE Energy Conversion Congress and Exposition (ECCE)*. IEEE, sep 2016.

[9] R. Georgious, J. Garcia, M. Sumner, S. Saeed, and P. Garcia, "Fault ride-through power electronic topologies for hybrid energy storage systems," *Energies*, vol. 13, no. 1, p. 257, jan 2020.

[10] Na Su, Dehong Xu, Min Chen, and Junbing Tao, "Study of bi-directional buck-boost converter with different control methods," in *2008 IEEE Vehicle Power and Propulsion Conference*. IEEE, sep 2008, pp. 1–5.

[11] C.-L. Wei, C.-H. Chen, K.-C. Wu, and I.-T. Ko, "Design of an average-current-mode noninverting buck–boost DC–DC converter with reduced switching and conduction losses," *IEEE Transactions on Power Electronics*, vol. 27, no. 12, pp. 4934–4943, dec 2012.

[12] Y.-J. Lee, A. Khaligh, and A. Emadi, "A compensation technique for smooth transitions in non-inverting buck-boost converter," in *2009 Twenty-Fourth Annual IEEE Applied Power Electronics Conference and Exposition*. IEEE, feb 2009.

[13] I. Aharon, A. Kuperman, and D. Shmilovitz, "Analysis of dual-carrier modulator for bidirectional noninverting buck–boost converter," *IEEE Transactions on Power Electronics*, vol. 30, no. 2, pp. 840–848, feb 2015.

[14] A. R. Borges and I. Barbi, "Three-phase single stage AC-DC buck-boost converter operating in buck and boost modes," in *XI Brazilian Power Electronics Conference*. IEEE, sep 2011.

[15] Y. Tang, Y. He, X. Dong, and S. Xie, "Research of a single-stage buck-boost inverter under dual mode modulation," in *IECON 2013 - 39th Annual Conference of the IEEE Industrial Electronics Society*. IEEE, nov 2013.

[16] Y. Tang, F. Xu, Y. Bai, and Y. He, "Comparative analysis of two modulation strategies for an active buck–boost inverter," *IEEE Transactions on Power Electronics*, vol. 31, no. 11, pp. 7963–7971, nov 2016.

[17] C.-H. Chen, C.-L. Wei, and K.-C. Wu, "Integrated non-inverting buck-boost DC-DC converter with average-current-mode control," in *2012 IEEE International Conference on Circuits and Systems (ICCAS)*. IEEE, oct 2012.

[18] C.-W. Chang and C.-L. Wei, "Single-inductor four-switch non-inverting buck-boost dc-dc converter," in *Proceedings of 2011 International Symposium on VLSI Design, Automation and Test*. IEEE, apr 2011.

[19] N. Zhang, S. Batternally, K. C. Lim, K. W. See, and F. Han, "Analysis of the non-inverting buck-boost converter with four-mode control method," in *IECON 2017 - 43rd Annual Conference of the IEEE Industrial Electronics Society*. IEEE, oct 2017.

[20] O. N. Almasi, V. Fereshtehpoor, M. H. Khooban, and F. Blaabjerg, "Analysis, control and design of a non-inverting buck-boost converter: A bump-less two-level t–s fuzzy PI control," *ISA Transactions*, vol. 67, pp. 515–527, mar 2017.